

From Disorder to Normal Rhythm: Traveling-Wave Control of Cardiac Arrhythmias

Rupamanjari Majumder^{1,*}, Vladimir S. Zykov^{1,†} and Eberhard Bodenschatz^{1,2,3,‡}

¹Max Planck Institute for Dynamics and Self-Organization, Göttingen, Germany

²Institute for Dynamics of Complex Systems, University of Göttingen, Göttingen D-37073, Germany

³Laboratory of Atomic and Solid-State Physics and Sibley School of Mechanical and Aerospace Engineering, Cornell University, Ithaca, New York 14853, USA

(Received 21 October 2021; revised 25 January 2022; accepted 5 May 2022; published 16 June 2022)

Lethal cardiac arrhythmias often involve the occurrence of spiral waves, whose control is essential for the treatment of the disease. While high-voltage shock-based control methods rely on ensuring an abrupt electrical synchronization of the heart, low-energy techniques mostly cause drift-induced termination of these waves. In particular, such a drift can be induced by a spatiotemporal modulation of domain excitability in optogenetically modified cardiac tissue. Here we demonstrate a low-energy optogenetics-based approach to suppress spiral waves via their transient chaotization and rapid drift.

DOI: 10.1103/PhysRevApplied.17.064033

I. INTRODUCTION

Self-organization of microscopic components often results in the emergence of fundamental universalities in complex excitable systems. A demonstration of such dynamic ordering, is the formation of spiral waves. These waves are typically associated with an ongoing physical process, e.g., morphogenesis in slime mold [1], spreading depression in the chicken retina [2], chemical reactions in the bulk or on surfaces [3–6], and fatal heart rhythm disturbances, known as arrhythmias [7]. Fast arrhythmias are generally associated with the occurrence of periodic, quasiperiodic, or chaotically rotating spiral waves that tend to override the normal pacemaker activity of the heart, resulting in inefficient pump function and a predisposition to sudden cardiac death. Restoration of normal cardiac activity requires the effective termination of these waves, which can only be achieved by eliminating the phase singularities (PSs) located at the spiral tips. According to nonlinear dynamics, this elimination is possible if and only if a PS collides with (i) an inexcitable boundary of the domain (where it is absorbed), or (ii) with another PS of opposite topological charge. Thus, an effective spiral-wave

termination strategy usually relies on a detailed knowledge of the precise location of the spiral tip, which can then be manipulated accordingly in favor of termination.

Manipulation of the spiral tip can be accomplished by modulating the excitability of the supporting domain. Studies show that such modulation can lead to drift [8–10], deformation [11], block [11], meander [8,12], breakup [11, 13], and even suppression of spiral waves [14–16]. Thus, this concept provides a framework for the development of advanced spiral-wave control strategies.

Here we present a fully automated, low-energy-based method for controlling spiral waves in simulated human atrial tissue. Our method is an invaluable improvement over previous approaches as it eliminates the need to know the exact position and dynamics of the spiral tip.

Our approach is inspired by the findings of Zykov *et al.* [9], who observed termination of spiral waves in Belousov-Zhabotinsky reaction systems by applying low-amplitude traveling-wave perturbations to the spiral wave. These perturbations induced slow and uncontrolled drift that eventually led to spiral-wave termination. To date, technical limitations made it difficult to test this theory in experiments. With the advent of cardiac optogenetics, it became possible to incorporate photosensitivity into otherwise light-insensitive cardiac tissue through genetic modification. This enables the modulation of cardiac tissue excitability by controlling the degree of membrane voltage depolarization using light of specific wavelengths and intensities [15–24] at submillimeter spatial precision and a temporal precision of a few milliseconds. Therefore, we anticipate that the approach presented in Ref. [9] might be possible to implement using cardiac optogenetics.

*rupamanjari.majumder@ds.mpg.de

†vladimir.zykov@ds.mpg.de

‡eberhard.bodenschatz@ds.mpg.de

Published by the American Physical Society under the terms of the [Creative Commons Attribution 4.0 International license](#). Further distribution of this work must maintain attribution to the author(s) and the published article's title, journal citation, and DOI. Open access publication funded by the Max Planck Society.

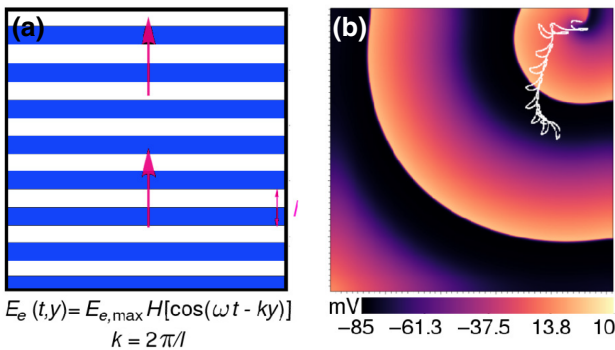


FIG. 1. (a) Spatiotemporal pattern of subthreshold illumination applied to the 2D domain containing the spiral wave. Blue stripes indicate areas where the light is applied; white stripes represent the nonilluminated regions. Pink arrows indicate the direction of movement of the stripes. The wavelength (l) of the stripes is associated with the wave number k as $k = \frac{2\pi}{l}$. (b) Spiral wave drift when applying the light pattern shown in (a), at $E_{e,\max} = 0.08 \text{ mW/mm}^2$, $\omega = 13.19 \text{ ms}^{-1}$, and $l = 1.056 \text{ cm}$.

In our simulations, we observe not only the drift of spiral waves as in Ref. [9] but also a process of rapid and effective termination of these waves by a mechanism that has not been reported before. The termination of spiral waves follows a transient fibrillatory state characterized by the controlled formation of wave breaks at several points in the spiral itself. Even in a tissue much larger than that of the human heart, this transient state lasts for $< 2 \text{ s}$, which is an order of magnitude shorter than the typical duration of a brief, nonfatal episode of atrial fibrillation (AF), i.e., 15–20 s [25]. Thus, we present a whole different approach to controlling spiral waves in a fast, effective, and robust manner.

II. METHODS

The electrical activity in human atrial tissue is modeled based on ion transport across cell membranes of connected cardiac cells, which are assumed to communicate

with their nearest neighbors via diffusive coupling. Consequently, the transmembrane potential (V) that developed across each cardiac cell membrane could be formulated using the following reaction-diffusion type equation:

$$\frac{dV}{dt} = \mathcal{D} \nabla^2 V - \frac{I_{\text{ion}}}{C_m}. \quad (1)$$

Here C_m is the capacitance of the cell membrane, \mathcal{D} is the diffusion coefficient for intercellular coupling, and I_{ion} is the total ionic current produced by each individual cell, formulated according to the Courtemanche-Ramirez-Nattel (CRN) model [26]. The model parameters are first adjusted to fit the action potential of the normal atrial working myocardium [27], and then altered according to Refs. [28–30] to obtain the diseased state of chronic AF (CAF) remodeling.

Photosensitivity is incorporated into the resulting cardiac cells by appending a four-state model for voltage- and light-sensitive Channelrhodopsin-2 [31] to the CRN CAF model. Thus Eq. (1) is updated as Eq. (2).

$$\frac{dV}{dt} = \mathcal{D} \nabla^2 V - \frac{I_{\text{ion}} + I_{\text{ChR2}}}{C_m}. \quad (2)$$

Here I_{ChR2} is the photocurrent produced by the Channelrhodopsin-2 ion channel. We use a maximum conductance value of $g_{\text{ChR2}} = 0.17 \text{ mS/cm}^2$ [22] for the I_{ChR2} channel, and express the irradiance of the applied light as E_e . For a detailed list of parameter values, we refer the reader to Ref. [31]. In order to impose spatiotemporal modulation of excitability, we apply moving zebra-like patterns over the spatial extent of the domain using Eq. (3):

$$E_e(t,y) = E_{e,\max} H[\cos(\omega t - ky)]. \quad (3)$$

Here $k = 2\pi/l$, where l is the wavelength of the propagating pattern, ω is the temporal frequency, and $H[z]$ is a Heaviside function. We find that for human atrial tissue, $E_{e,\max} = 0.095 \text{ mW/mm}^2$ marked the limit of subthreshold behavior. For simulations we use a time step of 0.02 ms and a grid spacing $\delta x = \delta y = 0.022 \text{ cm}$.

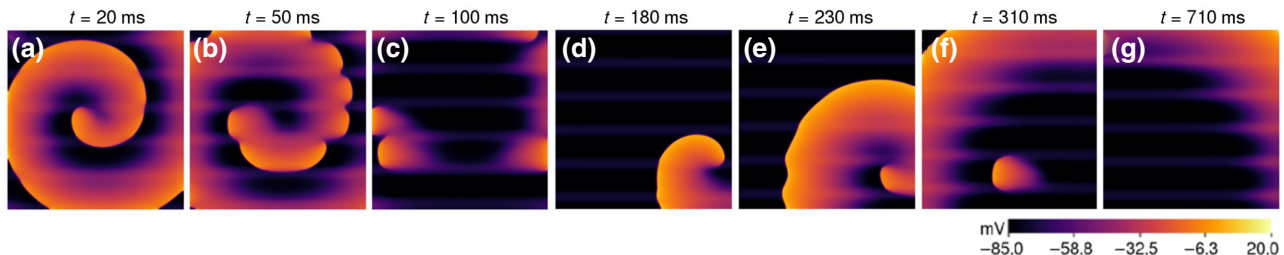


FIG. 2. Termination of spiral waves by transient breakup with spatiotemporal modulation of tissue excitability using the illumination pattern of Fig. 1(a) with $E_e = 0.092 \text{ mW/mm}^2$, $l = 2.112 \text{ cm}$, and $\omega = 12.56 \text{ ms}^{-1}$. (a) Initial state of the spiral. (b),(c) Formation of wave breaks at the interface between illuminated and nonilluminated stripes. (d),(e) Wave break evolves into another spiral, which anchors to an illuminated light stripe and is eventually eliminated after a few cycles (f),(g).

III. RESULTS

At low subthreshold light intensities moving zebra-like patterns [see Fig. 1(a)] induce spiral-wave drift in a manner similar to that observed by Zykow *et al.* [9] [see Fig. 1(b) and Video 1]. To shift the spiral wave close to the boundary, one needs to wait for more than ten rotational periods of the spiral. However, at high subthreshold intensity the same pattern causes rapid termination of the spiral through transient breakup [Figs. 2(a)–2(g) and Video 2]. Such breakup occurs consistently for a wide range of ω and k at $0.085 \text{ mW/mm}^2 < E_{e,\max} < 0.095 \text{ mW/mm}^2$ and is initiated along the interface between the illuminated and nonilluminated stripes [see, for example, Figs. 2(b) and 2(c)]. The other spiral tips, thus created, drift along the interface towards one of the inexcitable domain boundaries in favor of termination [Figs. 2(d)–2(g)].

To explain the mechanism of spiral-wave breakup in Fig. 2, we analyse the wave dynamics under subthreshold illumination in greater detail. In Fig. 3 we illuminate the top half of a square simulation domain ($22.53 \times 22.53 \text{ cm}^2$) with light of various subthreshold intensities ($E_e = 0.08, 0.085, 0.09, \text{ and } 0.092 \text{ mW/mm}^2$, respectively) and initiate a plane wave from the left edge of the domain. We note that the illumination has opposite effects on the wave front and wave back of the propagating wave [see Figs. 3(a1)–(a4) and 3(b1)–(b4)]. While the wave-front velocity increases slightly above normal ($\approx 9\%$ at $E_e = 0.092 \text{ mW/mm}^2$), the wave-back velocity is drastically reduced ($\approx 40\%$ at $E_e = 0.092 \text{ mW/mm}^2$), resulting in an effective extension of the spatial wavelength within the illuminated region. This changes the curvature of the wave front and wave back at the interface between the illuminated and nonilluminated regions. Figure 3(c) shows that applied illumination has a stronger impact on the conduction velocity (CV) restitution curve for the wave back, in comparison to the wave front. Furthermore, the strength of the impact correlates positively with the intensity of the applied illumination.

Next, we investigate the impact of “movement” of the light pattern on the wave front and the wave back of the propagating plane wave. To this purpose, we first illuminate the upper half of the $22.53 \times 22.53 \text{ cm}^2$ simulation domain for 180 ms. Then we shift the area of illumination upward by 30 grid points (0.66 cm) and observe the subsequent dynamics of the propagating wave. Our results reveal an immediate change in the curvature of the wave front and wave back at the interface between the illuminated and nonilluminated regions [see Fig. 3(d1)–(d4) for $E_e = 0.092 \text{ mW/mm}^2$]. While the wave front experiences a mild straightening upon removal of light (due to immediate restoration of the conduction velocity), the wave-back curvature changes from convex to concave, with stronger bending at higher light intensity. Simultaneously, at the

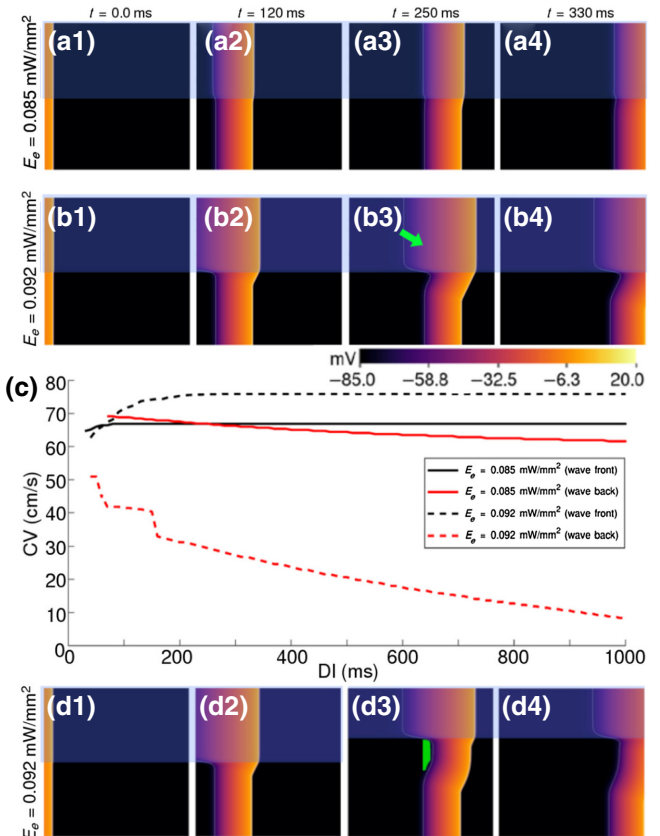


FIG. 3. Impact of illumination on the wave front and wave back of a propagating plane wave. (a1),(b1),(d1) A line stimulus is applied to the left boundary of the domain. (a2),(b2),(d2) The morphology of the wave after 120 ms in the presence of light. (a3)–(a4), (b3)–(b4) Difference in wave-front and wave-back velocities induces a curvature at the interface between the illuminated and nonilluminated regions (bold green arrow). (c) Conduction velocity restitution curves for wave front (black) and wave back (red) of the propagating wave. If the area of illumination is shifted, an excitation window emerges (d3) for $E_e = 0.092 \text{ mW/mm}^2$ (solid green area). (d4) Further propagation of the wave preserves the changed shape of the wave back. In (a),(b),(d) the illuminated region is marked using an overlaid transparent blue rectangle.

alternative location of the interface, we observe changing curvatures of the wave front and back as reported in Fig. 3(b1)–(b4). This leads to the emergence of an excitation window at high subthreshold light intensities [see Fig. 3 (d3)–(d4)].

Finally, we reproduce the simulation in Fig. 3(d) on a simulation domain containing a spiral wave. We observe that at $E_e = 0.092 \text{ mW/mm}^2$, the spiral develops wave breaks. In Fig. 4, we demonstrate the process for one such wave-break formation. Here, the break forms along the interface between the illuminated and nonilluminated regions. However, the alternative spiral wave establishes away from the interface. If we now consider a simulation

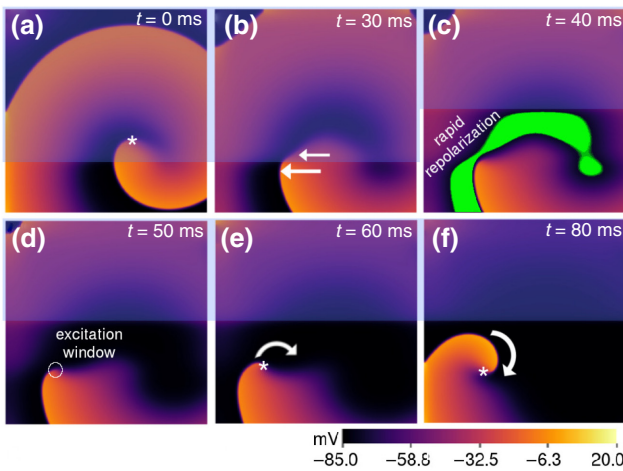


FIG. 4. Formation of a wave break on a spiral wave. Subfigure (a) shows the original location of the phase singularity at the spiral tip (white asterisk). (b) Application of light (overlaid transparent blue rectangle in each subfigure), induces a growing difference in the wave-front and wave-back velocities (bold white arrows) across the illumination interface. Strong wave front to wave back interactions result in a temporary conduction block in the illuminated region. (c) Shifting of the illumination pattern causes rapid repolarization of the region that previously contained the wave back, thereby releasing a large area of tissue (green) for re-excitation. (d) An excitation window emerges and an alternative phase singularity is developed (white circle), which establishes another spiral wave at the location of the wave break (e),(f).

domain in which a nonilluminated region is “sandwiched” between two illuminated regions (top and bottom), then as the illuminated pattern continues to shift, the formed spiral tip finds itself in the vicinity of the lower interface. Subsequently, the spiral anchors to the interface and is forced to move (along the interface) towards an inexcitable boundary for termination.

Our studies show that light stripes with low wave number and width > 2 cm, moving at temporal frequencies ($\simeq 1, 2$, or 5 Hz) slower than the rotation frequency of the spiral (i.e., $\simeq 8$ Hz) promote rapid termination of the spiral via the mechanism discussed. At frequencies ≥ 10 Hz, the same stripes lead to spiral-wave termination via wave breaking and overdrive pacing, with the latter taking predominance. Light stripes ≤ 1.0 cm may induce wave breaks and termination if they are moved sufficiently slowly ($\simeq 1$ Hz). However, at high temporal frequencies, these stripes have negligible influence on the dynamics of the spiral. These results are presented together in Video 3 for clear comparison.

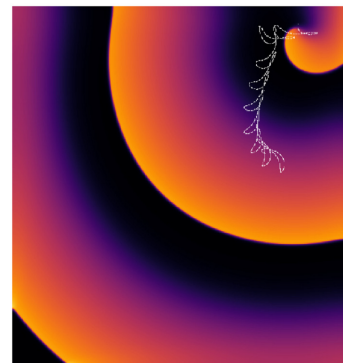
Finally, we check if the observations presented in Fig. 2 still hold for large system sizes and heterogeneous simulation domains. We find that our protocol successfully eliminates multiple spiral waves from a very large simulation domain (45.06×45.06 cm 2) (see Video 4), as

well as a single spiral wave from a 11.26×11.26 cm 2 domain with natural cellular heterogeneity and 20% diffuse fibrosis (Video 5). These results prove the robustness and efficacy of the method of spiral-wave termination via transient breakup in cardiac tissue systems using subthreshold optogenetics.

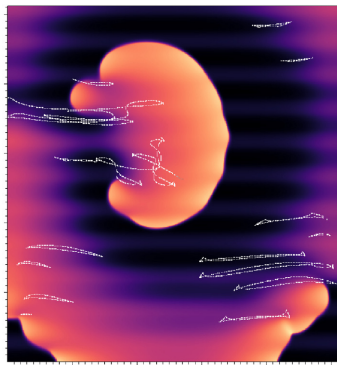
In summary, we present a consistent and effective approach to remove electrical spiral waves from excitable cardiac tissue by structured spatiotemporal modulation of tissue excitability. We use a series of traveling illumination stripes on optogenetically modified cardiac tissue at high, subthreshold light intensities to create transient disorder that eventually serves to control spiral-wave activity. The duration of this transient is much shorter than a very brief, nonlethal burst of fibrillatory activity. Such a system can be produced and studied in experiments. We find that the occurrence of “controlled” wave breaks in this system is crucial to the robustness of this method, because without them one would have to rely on drift-induced termination, which is a much slower and uncontrolled process.

IV. DISCUSSION

Despite the existence of extensive literature on cardiac optogenetics at suprathreshold light intensities, very little is known and understood about how the tool works in the subthreshold regime [32–35]. In a recent study, Majumder *et al.* [33] demonstrated the occurrence of controlled wave breaks in a system with global periodic subthreshold perturbations. Here we show formation of controlled wave breaks in a system with traveling-wave perturbations. Whereas the earlier study aimed to affect the spiral wave at all points simultaneously, leading to the onset and disruption of synchronization—a mechanism that can be compared to an earlier study by Sridhar and Sinha [36]—here about 50% of the domain remains

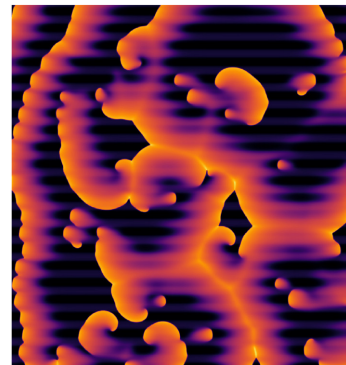


VIDEO 1. Drift of a spiral wave from the center of the 11.26×11.26 cm 2 simulation domain to an inexcitable boundary in favor of termination, using blue light stripes of width 1 cm, intensity $E_e = 0.08$ mW/mm 2 , and temporal frequency 2.1 Hz

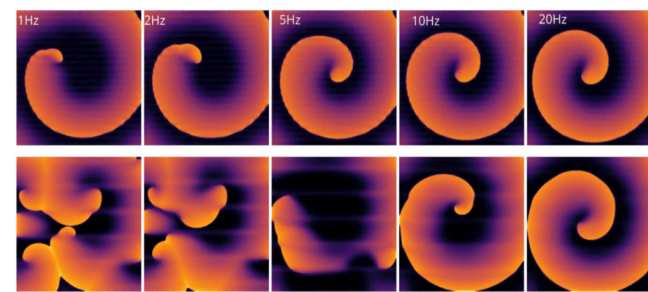


VIDEO 2. Breakup and termination of a spiral wave in an $11.26 \times 11.26 \text{ cm}^2$ simulation domain, using blue light stripes of width 1 cm, intensity $E_e = 0.092 \text{ mW/mm}^2$, and temporal frequency 5.0 Hz

nonilluminated at any point in time. Therefore, global synchronization can never occur. However, as in Ref. [33], there is a correlation between the times at which the wave breaks occur and the time at which the illumination undergoes a state change (*on-off* or vice versa). This suggests that the formation of controlled wave breaks is a local phenomenon that is triggered by the change in the state of illumination. In most complex excitable systems, modulation of excitability results in drift of spiral waves. This modulation can be spatial, temporal, or both [37], and can be enforced by a variety of means (optical, electrical, thermal, using ultrasound etc.), with or without feedback [38–40]. On the other hand, spiral wave break up is usually associated with parameter regimes that either induce some kind of memory effect in the dynamical system [41], or rely on the steepness of the slope, and/or dispersion of the action potential duration (APD) restitution curve properties within the domain [42,43]. Alternatively, one can expect to see spiral-wave breakup in a domain that supports supernormal excitability, as we have in our system. In the last case, as explained in Ref. [33], the occurrence of wave breaks is not related to the steepness or dispersion



VIDEO 4. Termination of multiple spiral waves in a $45.06 \times 45.06 \text{ cm}^2$ simulation domain using light stripes (width = 1 cm, temporal frequency 5 Hz, and $E_e = 0.092 \text{ mW/mm}^2$). The initial condition is obtained by periodically pulsing a single spiral wave in the domain, with global subthreshold illumination ($E_e = 0.093 \text{ mW/mm}^2$, temporal frequency = 1.2 Hz), for 3 s. After 3 s, the system is allowed to evolve for another 1 s before the traveling-wave protocol is initiated. Time $t = 0$ marks the beginning of the traveling-wave protocol.



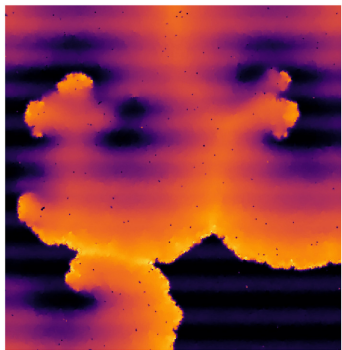
VIDEO 3. Comparison of the effect of traveling light stripes of the same width, applied to the same spiral initial condition, at varying temporal frequencies (1, 2, 5, 10, and 20 Hz), for two different wave numbers.

of the APD or CV restitution curves. Rather, it is the difference in CV restitution behavior of the wave front and wave back at different light intensities that plays a role.

V. OUTLOOK AND CONCLUSION

To conclude, we present a robust method to suppress spiral-wave activity without prior information about the location and dynamics of the spiral core. Our study demonstrates the possibility to ensure spiral-wave termination in a human atrial fibrillation model, using optogenetics at subthreshold light intensities. The method is based on the application of a spatiotemporal modulation of the medium parameters in the form of a moving zebra-like pattern that introduces a transient chaotic state that lasts for approximately equal to 1–2 s. During this time, electrical interactions between the existing activity within the domain and light-induced inhomogeneity caused by the projected light pattern results in co-ordinated suppression of the spiral wave at time scales, which are much smaller than those associated with conventional drift-induced termination. Here, note that (i) the duration of the chaotic transient is shorter than that of a nonlethal fibrillatory burst; (ii) the transient chaotic phase is marked by the occurrence of wave breaks in a self-organized manner that improves the efficiency of spiral-wave suppression; and (iii) the implementation of the method is also physically possible, for example, for optogenetically modified hearts using arrays of closely spaced micro-LEDs arranged on meshes surrounding the heart, which are capable of illuminating the heart from apex to base using illumination [44].

VI. VIDEO CAPTIONS



VIDEO 5. Termination of a single spiral wave in an $11.26 \times 11.26 \text{ cm}^2$ simulation domain containing natural cellular heterogeneity and 20% fibrosis, using traveling light stripes ($E_e = 0.092 \text{ mW/mm}^2$, width = 1 cm, and temporal frequency 5 Hz.)

ACKNOWLEDGMENTS

This work is supported by the Max Planck Society and the German Center for Cardiovascular Research (DZHK).

- [1] E. Pálsson and E. C. Cox, Origin and evolution of circular waves and spirals in *dictyostelium discoideum* territories, *Proc. Natl. Acad. Sci. USA* **93**, 1151 (1996).
- [2] N. A. Gorelova and J. Bureš, Spiral waves of spreading depression in the isolated chicken retina, *J. Neurobiol.* **14**, 353 (1983).
- [3] B. P. Belousov, in *Oscillations and traveling waves in chemical systems.*, edited by R. J. Field and M. Burger (Wiley, New York, 1985).
- [4] A. M. Zhabotinsky, A history of chemical oscillations and waves, *Chaos* **1**, 379 (1991).
- [5] M. Bär, N. Gottschalk, M. Eiswirth, and G. Ertl, Spiral waves in a surface reaction: Model calculations, *J. Chem. Phys.* **100**, 1202 (1994).
- [6] S. Jakubith, H. H. Rotermund, W. Engel, A. von Oertzen, and G. Ertl, Spatiotemporal Concentration Patterns in a Surface Reaction: Propagating and Standing Waves, Rotating Spirals, and Turbulence, *Phys. Rev. Lett.* **65**, 3013 (1990).
- [7] J. M. Davidenko, P. Kent, D. R. Chialvo, D. C. Michaels, and J. Jalife, Sustained vortex-like waves in normal isolated ventricular muscle, *Proc. Natl. Acad. Sci. USA* **87**, 8785 (1990).
- [8] S. Grill, V. S. Zykov, and S. C. Müller, Spiral wave dynamics under pulsatory modulation of excitability, *J. Phys. Chem.* **100**, 19082 (1996).
- [9] S. Zykov, V. S. Zykov, and V. Davydov, Spiral wave dynamics under traveling-wave modulation of excitable media, *Europhys. Lett.* **73**, 335 (2006).
- [10] L. Xu, Z. Li, Z. Qu, and Z. Di, Resonance drifts of spiral waves on media of periodic excitability, *Phys. Rev. E Stat. Nonlinear Soft Matter Phys.* **85**, 046216 (2012).
- [11] J. Ramos, Dynamics of spiral waves in excitable media with local time-periodic modulation, *Chaos Solitons Fractals* **13**, 1383 (2002).
- [12] O. Steinbock, V. Zykov, and S. Müller, Control of spiral-wave dynamics in active media by periodic modulation of excitability, *Nature* **366**, 322 (1993).
- [13] A. Schrader, M. Braune, and H. Engel, Dynamics of spiral waves in excitable media subjected to external periodic forcing, *Phys. Rev. E* **52**, 98 (1995).
- [14] J. Ma, C.-N. Wang, J. Tang, and Y.-F. Xia, Suppression of the spiral wave and turbulence in the excitability-modulated media, *Int. J. Theor. Phys.* **48**, 150 (2009).
- [15] R. Majumder, I. Feola, A. S. Teplinen, A. A. de Vries, A. V. Panfilov, and D. A. Pijnappels, Optogenetics enables real-time spatiotemporal control over spiral wave dynamics in an excitable cardiac system, *eLife* **7**, e41076 (2018).
- [16] R. Majumder, V. S. Zykov, and A. V. Panfilov, In silico optical control of pinned electrical vortices in an excitable biological medium, *New J. Phys.* **22**, 023034 (2020).
- [17] K. Deisseroth, Optogenetics, *Nat. Methods* **8**, 26 (2011).
- [18] Z. Jia, V. Valiunas, Z. Lu, H. Bien, H. Liu, H. Wang, B. Rosati, P. Brink, I. Cohen, and E. Entcheva, Stimulating cardiac muscle by light: Cardiac optogenetics by cell delivery, *Circ Arrhythm Electrophysiol.* **4**, 753 (2011).
- [19] T. Bruegmann, D. Malan, M. Hesse, T. Beiert, C. Fuegemann, B. Fleischmann, and P. Sasse, Optogenetic control of heart muscle *in vitro* and *in vivo*, *Nat. Methods* **7**, 897 (2010).
- [20] B. Bingen, M. Engels, M. Schalij, W. Jangsanthong, Z. Neshati, I. Feola, D. Ypey, S. Askar, A. Panfilov, D. Pijnappels, and A. de Vries, Light-induced termination of spiral wave arrhythmias by optogenetic engineering of atrial cardiomyocytes, *Cardiovasc Res.* **104**, 194 (2014).
- [21] C. Crocini, C. Ferrantini, R. Coppini, M. Scardigli, P. Yan, L. Loew, G. Smith, E. Cerbai, C. Poggesi, F. Pavone, and L. Sacconi, Optogenetics design of mechanistically-based stimulation patterns for cardiac defibrillation, *Sci Rep.* **6**, 35628 (2016).
- [22] T. Bruegmann, P. Boyle, C. Vogt, T. Karathanos, H. Arevalo, B. Fleischmann, N. Trayanova, and P. Sasse, Optogenetic defibrillation terminates ventricular arrhythmia in mouse hearts and human simulations, *J. Clin. Invest.* **126**, 3894 (2016).
- [23] E. C. A. Nyns, A. Kip, C. I. Bart, J. J. Plomp, K. Zeppenfeld, M. Schalij, A. De Vries, and D. A. Pijnappels, Optogenetic termination of ventricular arrhythmias in the whole heart: Towards biological cardiac rhythm management, *Eur Heart J.* **38**(27), 2132 (2017).
- [24] T. Bruegmann, T. Beiert, C. Vogt, J. Schrickel, and P. Sasse, Optogenetic termination of atrial fibrillation in mice, *Cardiovasc Res.* **114**, 713 (2018).
- [25] S. Swiryn, M. V. Orlov, D. G. Benditt, J. P. DiMarco, D. M. Lloyd-Jones, E. Karst, F. Qu, M. T. Slawsky, M. Turkel, and A. L. Waldo, Clinical implications of brief device-detected atrial tachyarrhythmias in a cardiac rhythm management device population, *Circulation* **134**, 1130 (2016).
- [26] M. Courtemanche, R. J. Ramirez, and S. Nattel, Ionic mechanisms underlying human atrial action potential properties: Insights from a mathematical model, *Am. J. Physiol. Heart Circ. Physiol.* **275**, H301 (1998), pMID: 29586616.

- [27] C. Tobón, C. A. Ruiz-Villa, E. Heidenreich, L. Romero, F. Hornero, and J. Saiz, A three-dimensional human atrial model with fiber orientation. Electrograms and arrhythmic activation patterns relationship, *PLOS ONE* **8**, 1 (2013).
- [28] M. Courtemanche, R. J. Ramirez, and S. Nattel, Ionic targets for drug therapy and atrial fibrillation-induced electrical remodeling: Insights from a mathematical model, *Cardiovasc. Res.* **42**, 477 (1999).
- [29] S. V. Pandit, O. Berenfeld, J. M. Anumonwo, R. M. Zaritski, J. Kneller, S. Nattel, and J. Jalife, Ionic determinants of functional reentry in a 2-D model of human atrial cells during simulated chronic atrial fibrillation, *Biophys. J.* **88**, 3806 (2005).
- [30] H. Zhang, C. J. Garratt, J. Zhu, and A. V. Holden, Role of up-regulation of i_{K1} in action potential shortening associated with atrial fibrillation in humans, *Cardiovasc. Res.* **66**, 493 (2005).
- [31] J. C. Williams, J. Xu, Z. Lu, A. Klimas, X. Chen, C. M. Ambrosi, I. S. Cohen, and E. Entcheva, Computational optogenetics: Empirically-derived voltage- and light-sensitive channelrhodopsin-2 model, *PLoS Comput. Biol.* **9**, 1 (2013).
- [32] R. Burton, A. Klimas, C. Ambrosi, J. Tomek, A. Corbett, E. Entcheva, and G. Bub, Optical control of excitation waves in cardiac tissue, *Nat. Photonics* **9**, 813 (2015).
- [33] R. Majumder, S. Hussaini, V. S. Zykov, S. Luther, and E. Bodenschatz, Pulsed low-energy stimulation initiates electric turbulence in cardiac tissue, *PLoS Comput. Biol.* **17(10)**, e1009476 (2021).
- [34] S. Park, S. Lee, L. Tung, and D. Yue, Optical mapping of optogenetically shaped cardiac action potentials, *Sci. Rep.* **4**, 6125 (2014).
- [35] S. Hussaini, V. Venkatesan, V. Biasci, J. M. Romero Sepúlveda, R. A. Quiñonez Uribe, L. Sacconi, G. Bub, C. Richter, V. Krinsky, U. Parlitz, R. Majumder, and S. Luther, Drift and termination of spiral waves in optogenetically modified cardiac tissue at sub-threshold illumination, *eLife* **10**, e59954 (2021).
- [36] S. Sridhar and S. Sinha, Response to sub-threshold stimulus is enhanced by spatially heterogeneous activity, *Euro Phys. Lett.* **92**, 60006 (2010).
- [37] I. V. Biktasheva, D. Barkley, V. N. Biktashev, and A. J. Foulkes, Computation of the drift velocity of spiral waves using response functions, *Phys. Rev. E* **81**, 066202 (2010).
- [38] S. Grill, V. S. Zykov, and S. C. Müller, Feedback-Controlled Dynamics of Meandering Spiral Waves, *Phys. Rev. Lett.* **75**, 3368 (1995).
- [39] V. Zykov and H. Engel, Feedback-mediated control of spiral waves, *Phys. D: Nonlinear Phenom.* **199**, 243 (2004).
- [40] S. W. Morgan, I. V. Biktasheva, and V. N. Biktashev, Control of scroll-wave turbulence using resonant perturbations, *Phys. Rev. E* **78**, 046207 (2008).
- [41] F. Fenton, S. Evans, and H. Hastings, Memory in an Excitable Medium: A Mechanism for Spiral Wave Breakup in the Low-Excitability Limit, *Phys. Rev. Lett.* **83**, 3964 (1999).
- [42] C. Zemlin and A. Panfilov, Spiral waves in excitable media with negative restitution, *Phys. Rev. E* **63**, 041912 (2001).
- [43] I. Banville and R. Gray, Effect of action potential duration and conduction velocity restitution and their spatial dispersion on alternans and the stability of arrhythmias, *J. Cardiovasc. Electrophysiol.* **13**, 1141 (2002).
- [44] L. Diaz-Maue, J. Steinebach, and C. Richter, Patterned illumination techniques in optogenetics: An insight into decelerating murine hearts, *Front. Physiol.* **12**, 750535 (2022).